

# The microstructure changes in the grain refined Al-Si-Mg alloy with the electro hydro pulse treatment

K. H. Kim<sup>1</sup>, V. M. Tsurkin<sup>2\*</sup>, A. V. Sinchuk<sup>2</sup>, Z. Trojanová<sup>3</sup>

<sup>1</sup>Department of Light Metals, Korea Institute of Materials Science, 797 Changwondaero, Changwon, Korea

<sup>2</sup>Department of Pulse Methods of Fluid and Crystallizing Alloy Treatment, Institute of Pulse Processes and Technologies, the National Academy of Sciences of Ukraine, Oktyabrsky Av. 43A, 54018 Nikolaev, Ukraine

<sup>3</sup>Department of Physics of Materials, Faculty of Mathematics and Physics, Charles University in Prague, Ke Karlovu 5, 121 16 Prague 2, Czech Republic

Received 8 February 2012, received in revised form 28 September 2012, accepted 28 September 2012

## Abstract

Al-4%Ti master alloy was used to refine the microstructure of an A357 aluminium alloy. For higher efficiency of the inoculating process in the alloy a new method has been developed. Electro hydro pulse treatment (EHPT) is able to influence the size and distribution of the inoculating TiAl<sub>3</sub> intermetallic particles. The treated alloy exhibited better mechanical properties. Possible mechanisms of the EHPT and the grain refinement are discussed.

Key words: aluminium alloy, grain refinement, inoculation, cavitations, hydrodynamic flows

## 1. Introduction

Main disadvantages of aluminium alloys casting products are low strength and low plasticity. Refining of the microstructure is one way how to solve this problem. In the last decades, the chemical inoculation has been used for the grain refinement of aluminium alloys. The state-of-the-art grain refinement practice involves addition of some master alloys (for example from the Al-Ti, Al-Ti-B, Al-Ti-C systems) before casting and introducing inoculating particles to the melt. These particles act as nucleation centres for  $\alpha$ -Al grains, resulting in a uniformly fine and equiaxed as cast microstructure. Papers [1, 2] review substantial information concerning the grain refinement by inoculants, the types of grain refiner and their manufacturing methods, the mechanisms of grain refinement, the fading and poisoning phenomena, and the trends in the development of new grain refiners for aluminium alloys. However, despite of the wide use of these methods, their physical base is not fully understood because the grain refinement efficiency depends on many factors. For example, Schumacher et al. [3] showed that the nucleation in an alloy using the grain refiners could be related to various effects, such as contact time of particles with the melt, possible fading,

and influence of the titanium content or the poisoning. For the efficient influence of refiners it is necessary to ensure that the inoculating particles are at the moment of solidification active enough and uniformly spread in whole volume. In many cases certain part of particles sediments on the bottom of a crucible and does not participate in the inoculation process. Experimental results presented in [4] showed that the overall particles sedimentation was mainly influenced by the particles size and distribution in the used master alloys and their agglomeration and dissolution properties in the liquid Al.

The aim of this work was to improve the mechanical properties of an A357 aluminium alloy via the grain refinement. To realize this goal it was necessary to speed up the solidification process and to involve from the master alloy into the inoculation process maximum of the high-melting and compact-shaped particles of the size below 1  $\mu\text{m}$ .

## 2. Experimental procedure

The EHPT used in this study is schematically presented in Fig. 1a. In the EHPT apparatus the electric energy is at the beginning accumulated in the ca-

\*Corresponding author: tel.: +380 512587110; fax: +380 512226140; e-mail address: [iipt@iipt.com.ua](mailto:iipt@iipt.com.ua)

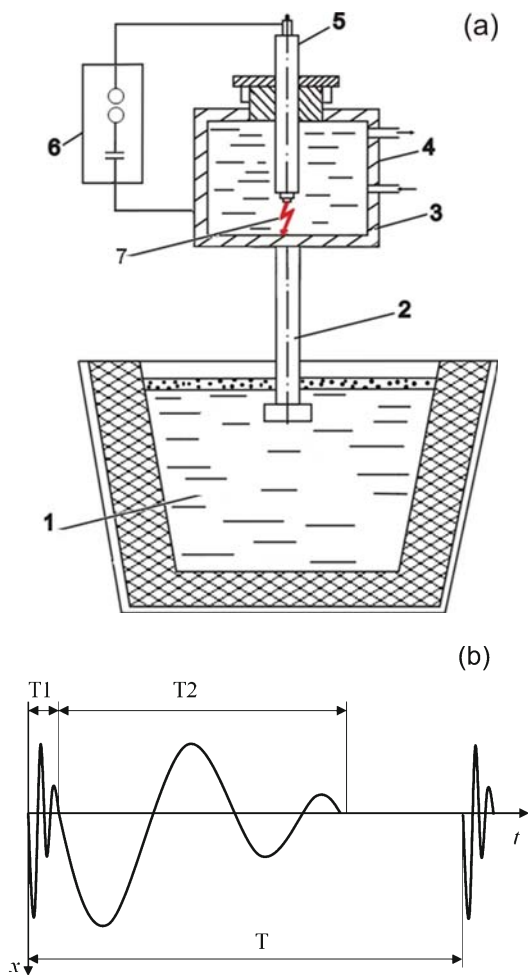


Fig. 1. Arrangement for EHPT: a) schematic diagram of the equipment: 1 – melt, 2 – waveguide, 3 – elastic membrane, 4 – discharge chamber with water, 5 – electrode, 6 – generator of pulse current, 7 – distance between electrodes; b) displacement of the waveguide bottom within duration of one pulse:  $T$  – duration of composite pulse,  $T_1$  – duration of the discharge period,  $T_2$  – duration of the post discharge period.

capacity store of the pulse current generator (6) and then suddenly (in  $\mu\text{s}$ ) released in a discharge chamber filled with the water (4) as a high-voltage discharge channel. The electric energy is transformed into the thermal one and dense low temperature plasma ( $10^4$  K) appears in the discharge channel. The pinch effect of the expanding plasma causes the movement of the waveguide top end (2). Oscillations of the waveguide are transmitted into the melt (1). In the following period the discharge channel is transformed into a pulsating vapour-gas cavity which deforms the elastic membrane (3) closing the bottom of the discharge chamber. These mechanical vibrations of the waveguide enter also into the melt. Duration of this second period is longer, approximately ms. The frequency of pulse repetition can be generated in the frequency interval from 1 to 20 Hz.

Following aluminium alloy was used in this study: 7.6%Si-1.25%Cu-0.4%Mg-0.25%Mn-0.5%Zn-1.0%Fe-balance Al. This is a Ukrainian analogue of the A357 alloy (according to ASTM designation). The Ukrainian standards ДСТУ 2839-94 admit slightly higher content of Cu and Fe comparing with the A357 alloy. Melting of the alloy was conducted in four graphite containers with similar volumes. Containers were preheated to  $750^\circ\text{C}$  for 30 min prior the finalization of the melting. Portion of Al-4%Ti master alloy (2.4–2.5 %) was added to each container for 5 min before completion of the melting. The containers with the melt were removed from the furnace stepwise while other containers remained inside of the furnace. The container with the melt was fixed on a heat-insulating support, then the waveguide was submerged into the melt at the crucible centre to the depth of 20 mm, and EHPT was carried out. When temperature decreased to  $T = 650^\circ\text{C}$ , the melt was cast into the steel moulding boxes to get cylindrical bars of diameter 20 mm and length 220 mm intended for studying structure and mechanical properties. During the experiment, temperature of the moulding box was held at  $300^\circ\text{C}$  and cooling rate of the melt was equal  $1^\circ\text{C s}^{-1}$ . Finally, the last container without EHPT was removed from the furnace and cooled naturally down to  $T = 650^\circ\text{C}$  and then cast into the moulding box. The time interval between the moment of extraction of the first and last fourth container with melt from the furnace made no more than 10 min. This allows us to speak about identity of temperature conditions of treatment and about nearly similar action of the modifier for each portion. Duration of the EHPT and the pulse exciting frequency were changed. The single pulse energy exhibited  $E_p = 1.25$  kJ and remained constant.

The sample surface was prepared using grinding and polishing procedure and etched in Keller solution (0.5 % HF in 50 ml  $\text{H}_2\text{O}$ ). Microstructure of castings was investigated with the light microscope Neophot-32M using standard techniques of a statistical microscopic metallography for calculation of average sizes of structural components. Uniaxial tension tests were performed at room temperature at an initial strain rate of  $2 \times 10^{-3} \text{ s}^{-1}$ . Samples were deformed either in as cast state or after the temper T6 (heating 1 h at  $535^\circ\text{C}$ , quenching into water of ambient temperature, then ageing annealing for 3 h at  $150^\circ\text{C}$ ). Electron-probe micro analyzer Superprobe-733 was used to estimate the resulting distribution of chemical elements in the treated samples.

### 3. Results and discussion

Figure 2 shows the microstructure of the samples without and with EHPT. Grain structure of all samples is typical for alloys subjected to grain refine-

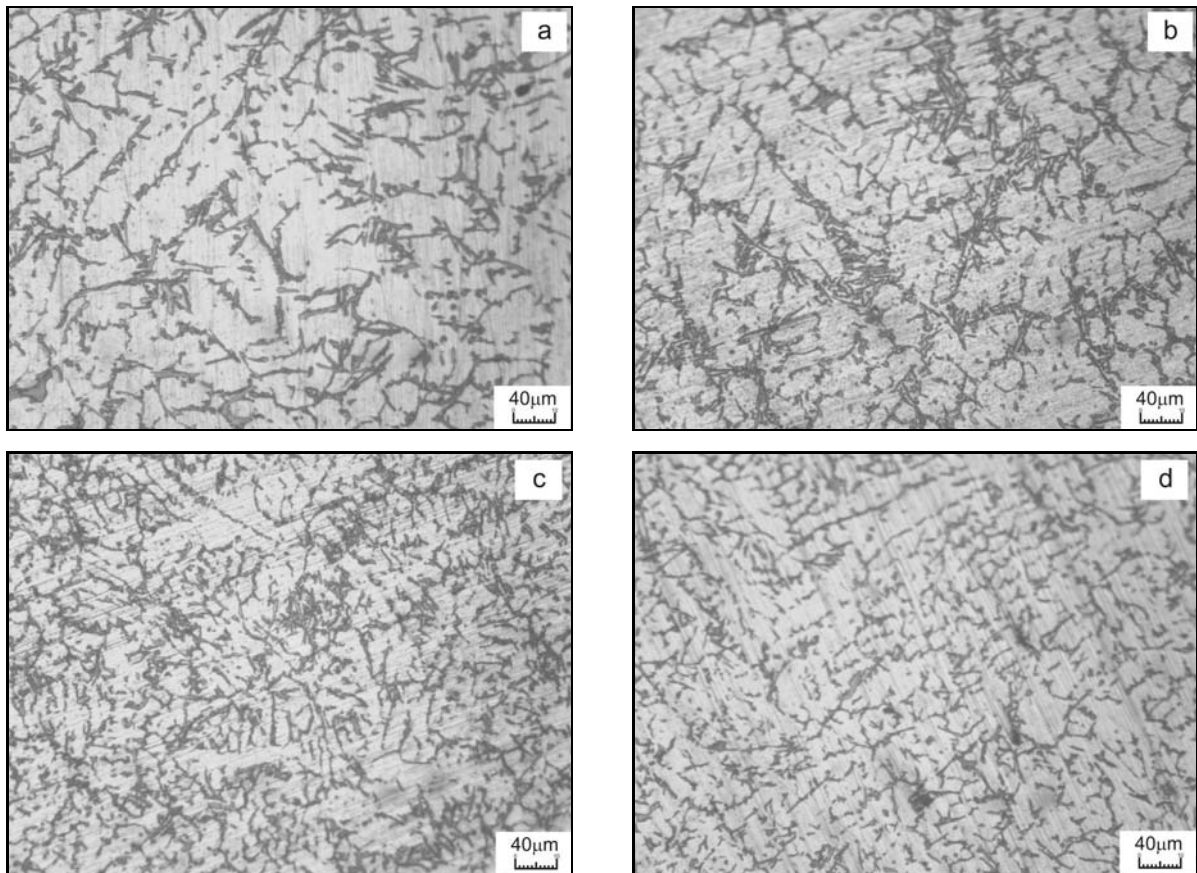


Fig. 2. Microstructure of the alloy without EHPT (a – sample 1) and with the EHPT (b, c, d – samples 2–4).

Table 1. Mechanical properties of the EHPT samples\*

Specimen Nr.	Duration of EHPT (min)	Frequency of pulse repetition (Hz)	UTS (MPa)	YTS (MPa)	Elong. (%)	Brinell hardness (MPa)
1	–	–	166 (195)	153 (161)	1.1 (1.7)	707 (835)
2	1.5	2	185 (228)	122 (151)	2.2 (3.6)	670 (810)
3	1.5	6	189 (231)	147 (164)	1.2 (2.6)	680 (810)
4	2.5	6	196 (216)	151 (187)	1.8 (1.2)	700 (880)
<b>mean after EHPT</b>	–	–	<b>190 (225)</b>	<b>140 (167)</b>	<b>1.7 (2.5)</b>	<b>683 (833)</b>

\*as cast (after T6)

ment. It is possible to see the transient degenerated dendrites mainly, which have not a clear orientation in space and in which arms of second and higher degree are absent. Doses of the EHPT for each sample are introduced in Table 1 together with the mechanical properties data. As it is obvious from Fig. 2, the higher doses of the EHPT, the finer the grain structure. Note that the amount of the master alloy was the same for all castings. The mean size of  $\alpha$ -grains in the sample Nr. 1 is 63  $\mu\text{m}$ ; in the sample Nr. 2 is 46  $\mu\text{m}$ , while in the samples Nr. 3 and Nr. 4 is nearly 30  $\mu\text{m}$ . Furthermore, a continuous increase of the ultimate tensile strength and elongation to fracture was

observed in the EHPT materials. Estimated values are higher than standard data for this alloy (according to Ukrainian standards, the ultimate tensile strength of the permanent-mould cast alloy AK7 should not be lower than 157 MPa and the elongation to fracture should be higher than 1.0 %, and the same alloy after the T6 temper should have the ultimate tensile strength not less than 196 MPa and the elongation to fracture higher than 0.5 %).

### 3.1. Grain refinement

The above introduced results may be explained

Table 2. Characteristics of TiAl<sub>3</sub> particles

Location	Content of TiAl <sub>3</sub> particles (vol.%)		Length of lamellar particles (μm)	Diameter of spherical particles (μm)
	lamellar	spherical		
In master alloy	12.3	0.1	28.2	12.3
In samples without EHPT	3.4	0.6	23.2	11.2
In samples after EHPT	0.8	1.0	16.9	9.3

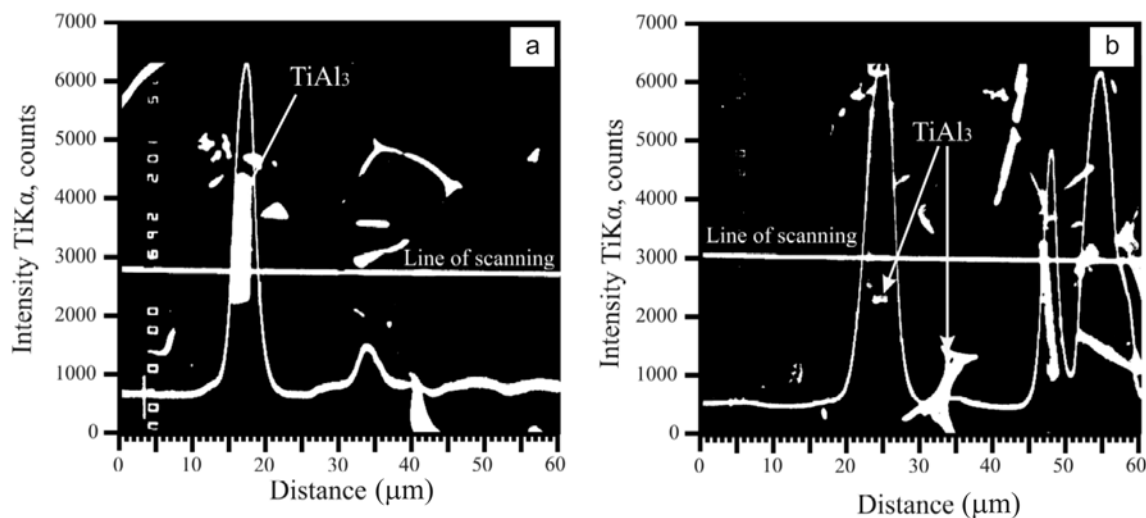


Fig. 3. The intensity of X-ray radiation describing Ti distribution along the scanning line: a) without EHPT, b) after EHPT.

taking into account the quantity and size of the inoculating particles inserted into the melt as the master alloy components. Titanium master alloy contains abundance of the rack-type intermetallic TiAl<sub>3</sub> particles. Their length is more than 10 μm and such big particles cannot naturally serve as nucleation sites for the α-phase grains. Characteristic sizes and shapes of the TiAl<sub>3</sub> particles present in the master alloy and in the alloy without and with the EHPT are introduced in Table 2. The content of TiAl<sub>3</sub> particles is substantially lower in the sample after EHPT. After the EHPT, the number of lamellar particles decreased, and the number of spherical particles increased 1.6 times. Mean diameter of the spherical particles decreased due to EHPT by 18 %, the length of lamellar particles – by 27 %. Figure 3 shows the radiation spectra which allowed observing the distribution of Ti atoms near the TiAl<sub>3</sub> particles. Micro-X-ray spectral analysis aided to establish the width of the Ti diffusion zone near the TiAl<sub>3</sub> particles showed the value 6.7 μm after the EHPT and 3.3 μm without the EHPT. This result indicates possible accelerated draw of atoms from the solid particles into the melt and confirms our idea that the EHPT intensifies the dissolving processes in the melt. During the solidification process a

higher number of particles become to be available to participate in the nucleation process.

### 3.2. Mechanisms of electro hydro pulse treatment

As can be seen from Fig. 1b, each of composite pressure pulses that enter into the melt during the EHPT has two basic stages. At the first stage the pressure of the plasma channel creates the wave process in the waveguide whose bottom end generates the non-stationary pressure field within the melt. The acoustic spectrum of such generated pulse was found in a wide range of the exciting frequencies (from units of Hz to 100 kHz). The magnitude of the acoustic pulse pressure entering into the melt was found to be about (10<sup>5</sup>–10<sup>6</sup>) Pa. Such pressure is high enough to overcome the cavity threshold opening stress for a metallic liquid, i.e. it is able to invoke acoustic cavities within the treated melt. Therefore, during the first discharge stage cavity bubbles fill with the dissolved hydrogen and also some other gases are formed in the melt. The bubbles stepwise grow or a coalescence of bubbles may occur. Bigger bubbles move up to the melt surface lugging by away light non-metallic inclusions. Remaining

bubbles in the melt oscillate under the stress produced by the acoustic field and collapse with the high velocity. As a result of the collapsed bubbles, powerful shock waves spread in the adjacent micro areas in the melt. This process was described with more details earlier in [5, 6]. If the collapse occurs near a particle or, what is more probable, directly on a particle, the particle can be under the action of the shock waves mechanically broken into smaller parts. Such smaller particles may be easily dissolved under the action of arising micro-streams of the liquid via the viscous friction.

In the second post-discharge stage where the plasma channel is transformed into the pulsating vapour-gas cavity the frequency spectrum of the exciting vibrations is narrower in comparison with the first stage – only from units of Hz to approximately 10 Hz. The amplitude of the waveguide movement during this stage is a few mm, and moving velocity from  $10^{-2}$  to  $10 \text{ m s}^{-1}$ . Motion of the waveguide end causes intensive hydrodynamic flows in the melt by which inoculating particles are spread in the whole volume. The chemical composition and temperature are homogenized in the material volume.

#### 4. Conclusion

Presented experimental data show that the grain refinement process (the master alloy dissolution, its fixation by the melt, compaction of inoculating

particles and their uniform distribution may proceed more efficiently applying the EHPT. The treated alloy exhibits finer grains and improved mechanical properties as compared to the alloy in which above mentioned processes proceed spontaneously. The observed electro hydro pulse influence on the inoculating particles may be connected with various acoustic effects, which are up to now not completely clear. The cavitations effects in the melt and hydrodynamic flows are very probably responsible for the improved properties of the alloy. Further studies will be necessary for the full explanation of processes occurring during the electro hydro pulse treatment.

#### References

- [1] Murty, B. S., Kori, S. A., Chakraborty, M.: *Inter. Mater. Rev.*, 47, 2002, p. 3.  
[doi:10.1179/095066001225001049](https://doi.org/10.1179/095066001225001049)
- [2] Qusted, T. E.: *Mater. Sci. Technol.*, 20, 2004, p. 1357.  
[doi:10.1179/026708304225022359](https://doi.org/10.1179/026708304225022359)
- [3] Schumacher, P., Greer, A. L., Worth, J., Evans, P. V., Kearns, M. A., Fisher, P., Green, A.: *Mater. Sci. Technol.*, 14, 1998, p. 394.  
[doi:10.1179/026708398790301241](https://doi.org/10.1179/026708398790301241)
- [4] Vinod Kumar, G. S., Murty, B. S., Chakraborty, M.: *Inter. J. Cast Met. Res.*, 23, 2010, p. 193.  
[doi:10.1179/136404610X12665088537491](https://doi.org/10.1179/136404610X12665088537491)
- [5] Tsurkin, V. N., Sinchuk, A. V.: *Casting Processes*, 1, 2004, p. 6.
- [6] Tsurkin, V. N., Sinchuk, A. V.: *Casting Processes*, 1–2, 2007, p. 70.